



## Preparation and properties of TS-1 zeolite and film using Sil-1 nanoparticles as seeds

Fangrui Qiu<sup>a</sup>, Xiaobin Wang<sup>a</sup>, Xiongfeng Zhang<sup>a,\*</sup>, Haiou Liu<sup>a</sup>, Shunqin Liu<sup>a</sup>, King Lun Yeung<sup>b,\*</sup>

<sup>a</sup> State Key Laboratory of Fine Chemicals, School of Chemical Engineering, Dalian University of Technology, No. 158 Zhong Shan Road, Dalian 116012, PR China

<sup>b</sup> Department of Chemical Engineering, the Hong Kong University of Science and Technology, Clear Water Bay, Kowloon, Hong Kong, SAR, PR China

### ARTICLE INFO

#### Article history:

Received 3 September 2008

Received in revised form

15 November 2008

Accepted 17 November 2008

#### Keywords:

Silicalite-1

TS-1

Zeolite

Film

Membrane reactor

### ABSTRACT

Titanium silicalite-1 (TS-1) zeolites and films supported on porous  $\alpha$ -Al<sub>2</sub>O<sub>3</sub> tubes were prepared using TS-1 and silicalite-1 (Sil-1) seeds by hydrothermal synthesis. The structure and catalytic properties of the TS-1 powders and films were characterized by SEM, XRD, FT-IR, UV-vis and styrene partial oxidation by hydrogen peroxide. The results showed that TS-1 prepared from Sil-1 seeds were as active as TS-1 from nucleated and TS-1 seeded syntheses, in spite of the concerns about nonuniformity and dilution caused by the use of pure silica Sil-1 seeds. The Ti atoms were successfully incorporated as tetra-coordinated titanium in the zeolite framework and the phenylacetaldehyde selectivity correlates well with the infrared band for Ti–O–Si of the TS-1. Reaction over TS-1 film indicates that reactions occurred at the topmost layer of the film due to the slow diffusion in the zeolite pores.

© 2008 Elsevier B.V. All rights reserved.

### 1. Introduction

Titanium silicalite-1 (TS-1) is an excellent selective oxidation catalyst for conversions of alkenes to epoxides, alcohols to aldehydes, alkanes to secondary alcohols and ketones, phenol to hydroquinone and pyrocatechol, and amines to hydroxylamines under mild reaction conditions using hydrogen peroxide as oxidant [1]. A good TS-1 catalyst is characterized by high framework titanium content with little or no extra-framework titanium [2]. And recent reports indicate that small TS-1 particles exhibit particularly high catalytic activity [3,4]. TS-1 zeolites are crystallized by hydrothermal process that often lasts between 3 and 10 days. The long crystallization time often leads to large TS-1 zeolite and formation of extra-framework titanium that lower the selectivity of the zeolite catalyst. Many researchers reported that adding seeds to the synthesis solution could decrease the zeolite crystal sizes, promote zeolite growth and improve their crystallization [5,6]. Lu and Wang [7] prepared micron-sized TS-1 zeolites using seeded growth by adding TS-1 seeds. Without seeding, no zeolite can be obtained from the same synthesis mixture even after 7 days. It is possible to nucleate seeds in situ before crystallization. This method was used to prepare TS-1 by preheating a silicate gel to generate MFI seeds before the addition of Ti precursor [8]. This approach considerably

speed-up the crystallization of TS-1. Cundy et al [9,10] studied the nucleation and growth of Sil-1 and TS-1 prepared by seeding and aging gel of precursor sols.

Reaction on catalytic thin film is of interest in many new reactor designs including catalytic membrane reactors [11–13] and microreactors [14–19]. Oriented TS-1 film was successfully grown on chitosan modified porous alumina [20] and on porous stainless steel tubes [21] for membrane reactor applications. The preparation and their performance of TS-1 films on microchannel reactor and tubular separator were investigated [4,22,23]. Selective oxidation of aniline to azoxybenzene over TS-1 catalyst was carried out in a membrane microreactor with a significant improvement in catalyst selectivity and life [24]. The thin zeolite film and membrane are often prepared by first pre-seeding the substrate with zeolite nanocrystals followed by a hydrothermal synthesis in either precursor solution or gel. This technique offers excellent control on the zeolite film orientation [25], morphology [26,27] and growth [28,29]. The zeolite-type, size, shape and orientation of the seeds are known to affect the zeolite film growth on surfaces [25,30–32]. It is common to prepare zeolite films and membranes from seeds of similar zeolite type, but this is difficult for TS-1 film as the TS-1 seeds of submicron size are difficult and expensive to prepare. However the use of Sil-1 seed could lead to nonuniform core-shell structure and dilute the titanium content that could affect the catalyst performance of the prepared zeolites. This work investigates the preparation and properties of TS-1 zeolites and films grown from TS-1 and Sil-1 seeds. The TS-1 zeolites and films were characterized by SEM, XRD, FT-IR and UV-vis and their catalytic property

\* Corresponding author. Tel.: +86 411 88993605; fax: +86 411 83633080.

E-mail addresses: [xfzhang@dlut.edu.cn](mailto:xfzhang@dlut.edu.cn) (X. Zhang), [kekyeung@ust.hk](mailto:kekyeung@ust.hk) (K.L. Yeung).

was evaluated for the selective oxidation of styrene to benzaldehyde and phenylacetaldehyde by hydrogen peroxide.

## 2. Experimental

### 2.1. Materials

Chemicals used in the zeolite synthesis and reaction experiment include analytical grade tetraethyl orthosilicate (TEOS), isopropyl alcohol (IPA), acetone, styrene and 30 wt% H<sub>2</sub>O<sub>2</sub> purchased from Tianjin Kermel Chemical Reagents Ltd. Co. The tetrabutyl orthotitanate (TBOT, AR grade) was supplied by Beijing Xingjin Chemical Reagent Co., while the tetrapropyl ammonium hydroxide (TPAOH, 27 wt%, aqueous) was synthesized in the laboratory. The  $\alpha$ -Al<sub>2</sub>O<sub>3</sub> tubes were supplied by Nanjing University of Technology and measured 13 mm O.D., 9 mm I.D. and 75 mm in length. The tubes have an average pore size of 0.5–1  $\mu$ m and a porosity of 30–40%.

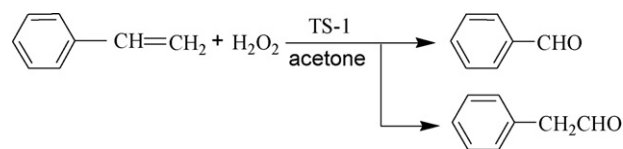
### 2.2. Preparation of TS-1 zeolite

The preparation of Sil-1 and TS-1 seeds was carried out according to the procedure reported in the literature [9,10,33]. The particle size of Sil-1 and TS-1 seeds was approximately 150 nm.

The TS-1 zeolite was prepared according to the procedure reported in a previous work by the authors [34]. The TPAOH was divided into two parts for hydrolysis of TEOS and TBOT. In a typical synthesis, 2 g TBOT was dissolved in 14 g IPA. 24 g of TPAOH (27 wt%, aqueous) and 26 g H<sub>2</sub>O were slowly added to the solution under stirring to give a solution A. Solution B was prepared by adding 31 g TEOS dropwise to a mixture of 14 g H<sub>2</sub>O and 10.4 g TPAOH under vigorous stirring. Solutions A and B were stirred for an additional 2 h to allow a full hydrolysis of the alkoxide reagents. Measured amount of solution A was added to solution B and the mixture was heated to 358 K in a water bath to evaporate the IPA and the alcohol produced by the hydrolysis of TEOS and TBOT. Deionized distilled water was added to make-up for the lost volume. A homogeneous solution with a molar composition of 1 TEOS: 0.04 TBOT: 0.32 TPAOH: 25 H<sub>2</sub>O was obtained after mixing for 24 h. Sil-1 or TS-1 seeds with an average diameter of 150 nm were then added (0.27 wt.% of the synthesis solution in the autoclave) and the mixture was stirred at room temperature for 1 h and sonicated for 5 min before transferring to a stainless steel autoclave for hydrothermal synthesis under static conditions at 448 K for 48 h. The synthesis was quenched by rapidly cooling the autoclave, and the zeolite was recovered by a series of centrifugation and washing steps. The zeolite was dried in an oven at 393 K for 12 h before calcining in air at 823 K for 6 h. The TS-1 zeolite powder prepared from Sil-1 and TS-1 seeds is referred to as S-TS-1 and T-TS-1, while N-TS-1 refers to TS-1 crystallized in the absence of seeds from the same synthesis mixture and condition as S-TS-1.

### 2.3. Preparation of TS-1 film

The TS-1 films supported on porous  $\alpha$ -Al<sub>2</sub>O<sub>3</sub> tubes were prepared using Sil-1 seeds. A 2 wt% Sil-1 sol in water was prepared according to the procedure reported in a previous work [26]. The porous  $\alpha$ -Al<sub>2</sub>O<sub>3</sub> tube was cut into 75 mm lengths, rinsed with deionized distilled water, dried at 373 K for 12 h before air calcination at 823 K for 6 h. A thin layer of Sil-1 seeds was coated onto the inner surface of the tubes by dip-coating in the Sil-1 sol for 40 s. The seeded tube was dried overnight at room temperature and calcined at 823 K for 6 h to obtain good seed adhesion. The outer surface of the seeded tube was wrapped with Teflon tape, placed in a 120 ml autoclave vessel and immersed in a clear synthesis solution with a molar composition of 1 TEOS: 0.04 TBOT: 0.32 TPAOH: 250 H<sub>2</sub>O. The zeolite film was grown at 448 K for a given time period. After



Scheme 1. Oxidation of styrene with hydrogen peroxide.

synthesis, the sample was rinsed with deionized distilled water, dried overnight at 333 K and calcined at a heating rate of 1 K/min to remove the organic templates. For comparison, the preparation of TS-1 film using TS-1 seeds was investigated by traditional secondary growth method. The TS-1 seeds were prepared from the same synthesis mixture as N-TS-1.

### 2.4. Characterization

The TS-1 zeolites and films were characterized by various methods. The zeolite structure was analyzed by D/Max 2400 Rigaku X-ray diffractometer with Cu-K $\alpha$  radiation ( $\lambda = 0.1542$  nm) and the crystal size and film morphology were examined by KYKY-2800B scanning electron microscope (SEM). The FT-IR spectra of the samples were recorded on a Bruker EQUINOX55 spectrometer using KBr pellet technique for powder and ATR (attenuated total reflectance) technique for the films. While the diffuse reflectance UV–vis spectra were obtained on a JASCO V-550 spectrometer with BaSO<sub>4</sub> for reference. The tubular samples were cut into smaller flat pieces for the UV–vis experiments.

### 2.5. Catalytic activity

The catalytic oxidation of styrene with hydrogen peroxide (Scheme 1) were carried out in a conventional batch reactor for TS-1 catalyst powders and in a laboratory membrane reactor shown in Fig. 1 for the catalytic TS-1 films. The batch reaction lasted for 5 h and samples were taken at regular intervals for analysis. The catalyst was separated from the reaction mixture by centrifugation. The ceramic tube coated with TS-1 thin film was sealed in the shell reactor and a heating tape was wrapped around the reactor to keep the temperature at 343 K. The reactants were fed from a reservoir flask fitted with a water-cooled condenser to prevent excessive liquid evaporation. Acetone, styrene and hydrogen peroxide in the molar composition of 4.62:1:0.33 were added to the three-neck reservoir flask under stirring. The reactant mixture was circulated by a pump to the reactor at a flow rate of 0.8 ml/min and samples were taken from the outlet (c.f. Fig. 1) at regular intervals.

The reactant and the product were analyzed by a gas chromatograph (GC7890F, Shanghai Techcomp Limited), with a capillary column (SE-30, 150 m  $\times$   $\emptyset$  0.32 mm  $\times$  0.5  $\mu$ m) using a flame ionization detector. The styrene conversion, product selectivity and yield were calculated:

$$\begin{aligned}
 X_{\text{STY}} &= \frac{n_{\text{BAL}} + n_{\text{PAC}} + n_{\text{others}}}{n_{\text{STY}} + n_{\text{BAL}} + n_{\text{PAC}} + n_{\text{others}}} \times 100\% \\
 S_{\text{PAC}} &= \frac{n_{\text{PAC}}}{n_{\text{BAL}} + n_{\text{PAC}} + n_{\text{others}}} \times 100\% \\
 S_{\text{BAL}} &= \frac{n_{\text{BAL}}}{n_{\text{BAL}} + n_{\text{PAC}} + n_{\text{others}}} \times 100\% \\
 S_{\text{AA}} &= S_{\text{PAC}} + S_{\text{BAL}} \\
 Y_{\text{PAC}} &= X_{\text{STY}} \times S_{\text{PAC}} \times 100
 \end{aligned} \quad (1)$$

where  $X$  is the conversion,  $S$  the selectivity,  $Y$  the yield,  $n$  the mol of the chemicals, STY styrene, BAL benzaldehyde, PAC phenylacetaldehyde, Others phenyl methyl ketone, tars styrene polymers and unidentified high boiling compounds, and AA aromatic aldehyde.

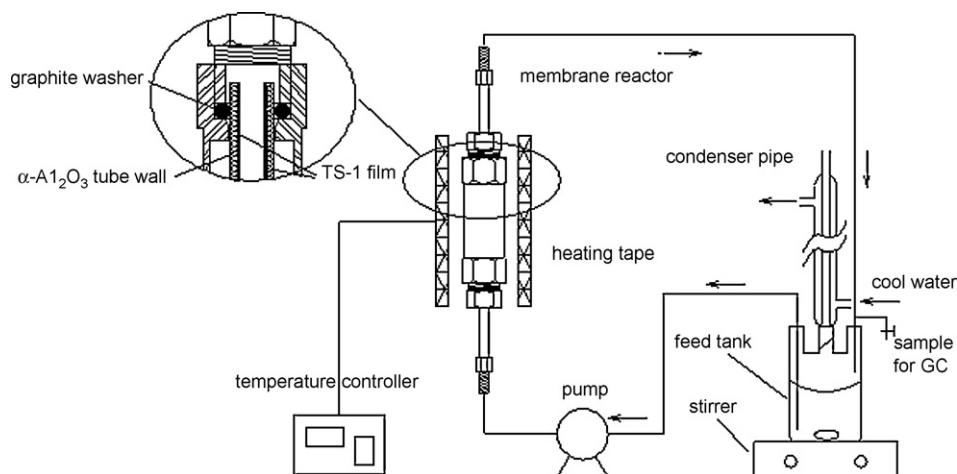


Fig. 1. Schematic of the reaction apparatus.

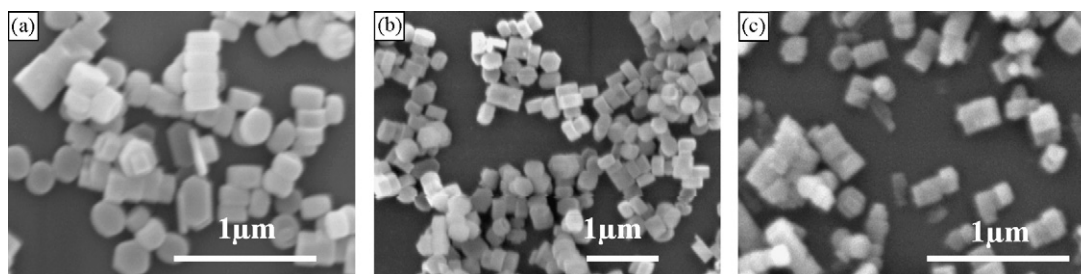


Fig. 2. SEM images of the synthesized TS-1 zeolites: (a) TS-1-48h without seed (N-TS-1), (b) TS-1-24h with TS-1 seeds (T-TS-1), and (c) TS-1-24h with silicalite-1 seeds (S-TS-1).

### 3. Results and discussion

#### 3.1. Preparation of TS-1 zeolite and film by silicalite-1 crystals as seeds

##### 3.1.1. TS-1 zeolite powders

The TS-1 zeolites prepared from Sil-1 seeds (S-TS-1) are morphologically indistinguishable from the TS-1 zeolites prepared without seeds (N-TS-1) as shown in Fig. 2. The N-TS-1 obtained after 48 h of crystallization has similar particle size as S-TS-1 grown from Sil-1 seed for 24 h. However, the particle size is smaller than the T-TS-1 prepared after 24 h of crystallization. The zeolite growth is faster for the seeded synthesis as expected, but unlike Lu and Wang [7], who reported large, aggregated TS-1 crystals from their seeded growth, there is no apparent aggregation in S-TS-1 and the sample shows well crystallized zeolites of regular size and shape. The average particle size of T-TS-1 sample is approximately 220 nm, while the S-TS-1 and N-TS-1 are around 160 nm and 180 nm, respectively. Lu and Wang [7] obtained larger TS-1 zeolites (i.e., 0.4–1.5 μm) from inorganic  $\text{TiCl}_3$  and silica sol precursors. They reported large micron-sized TS-1 zeolites were obtained from Sil-1 seeds, while smaller TS-1 were prepared from TS-1. The X-ray diffraction of N-TS-1, T-TS-1 and S-TS-1 are shown in Fig. 3. The diffraction peaks ( $2\theta = 7.9^\circ, 8.8^\circ, 23.1^\circ, 23.9^\circ, 24.4^\circ$ ) are consistent with that of the standard TS-1 zeolites and are characteristics of MFI with an orthorhombic symmetry [1].

The use of Sil-1 seeds for growing TS-1 could result in a nonuniform core-shell structure as well as the dilution of titanium content. Both could lead to poorer reaction performance as the amount of  $\text{Ti}^{4+}$  inserted into the zeolite framework is closely related to the catalytic property of TS-1 zeolite. The FT-IR spectra of N-TS-1, T-TS-1 and S-TS-1 shown in Fig. 4a are nearly identical and display infrared

peaks at 1220, 1100, 960, 800, 550 and 450  $\text{cm}^{-1}$ . The peaks at 550 and 450  $\text{cm}^{-1}$  belong to Si–O–Si rocking. The signal 800  $\text{cm}^{-1}$  is referred to the symmetric stretching/bending of Si–O–Si bridges and the peak at 1100  $\text{cm}^{-1}$  with a shoulder at 1220  $\text{cm}^{-1}$  is often assigned to the Si–O–Si asymmetric stretching [35]. These peaks are common in MFI zeolites. The absorption band at 960  $\text{cm}^{-1}$  is often assigned to Ti–O–Si and is taken as good indication of titanium substitution into the zeolite framework. The UV–vis spectra of the N-TS-1, T-TS-1 and S-TS-1 were also obtained and shown in Fig. 5a. The absorption band in the wavelength region of 210–220 nm is attributed to isolated Ti in zeolite the framework [36]. Both N-TS-

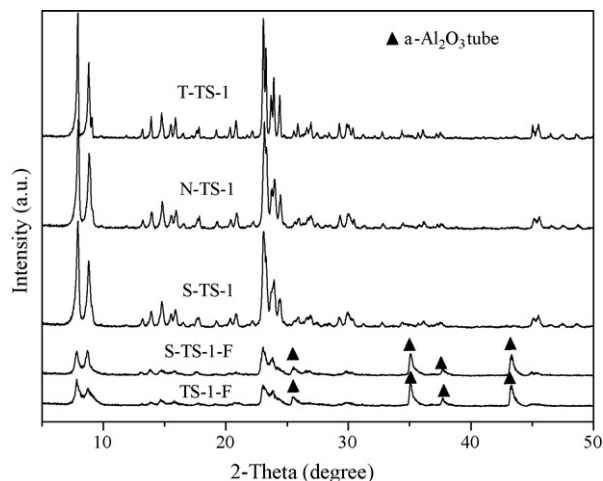


Fig. 3. XRD patterns of the TS-1 zeolites and films.

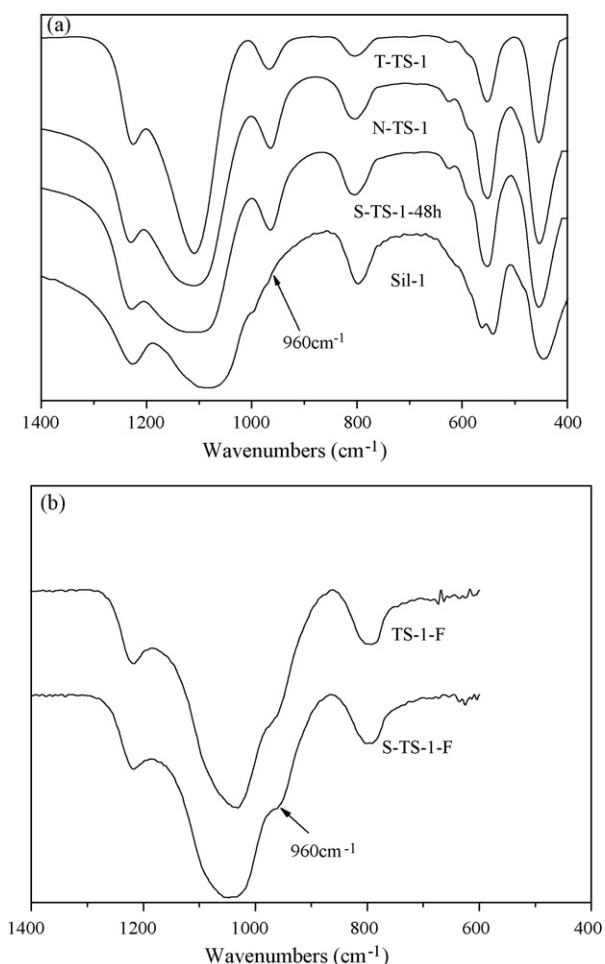


Fig. 4. FT-IR spectra of the TS-1 zeolites (a) and films (b).

1 and T-TS-1 have an absorption band at 220 nm. A slight peak shift to 215 nm was observed for S-TS-1 due to the Sil-1 seed. On the other hand, N-TS-1 displays weak signals at 270–280 nm and 330 nm that are assigned to hexa-coordinated Ti species and anatase TiO<sub>2</sub> [37,38] indicating the presence of extra-framework titanium.

The FT-IR and UV–vis spectra do not give evidence for a nonuniform Ti distribution in the S-TS-1 prepared from Sil-1 seeds. It is speculated that the Sil-1 seeds may partially dissolved under the alkaline pH (ca. pH 12) and form Si–O–Si oligomers at the high synthesis temperature (i.e., 448 K) contributing to the growth of TS-1 [39,40]. The oligomers might be reconstructed with the superfluous Ti species in the liquid phase, leading to the formation of titanosilicate species. Thus the additional Sil-1 seeds help to prevent the polymerizing of the redundant titanium species to hexa-coordinated Ti and anatase TiO<sub>2</sub>. Recently, Tamura et al. [40] also discovered the similar phenomena in studying the incorporation process of titanium species into the framework of MFI type zeolite by using silicalite-1 as a starting silica source.

### 3.1.2. TS-1 zeolite films

Synthesis carried out without seeds deposits mostly amorphous materials on the ceramic tube with few poorly crystallized zeolites. In general, it is more difficult to grow a continuous layer of zeolite film by in-situ hydrothermal synthesis [19]. Fig. 6 shows the ceramic supports after seeding with Sil-1 seeds and growing the TS-1 films on the seeded supports. Fig. 6a and b indicate that the surface is

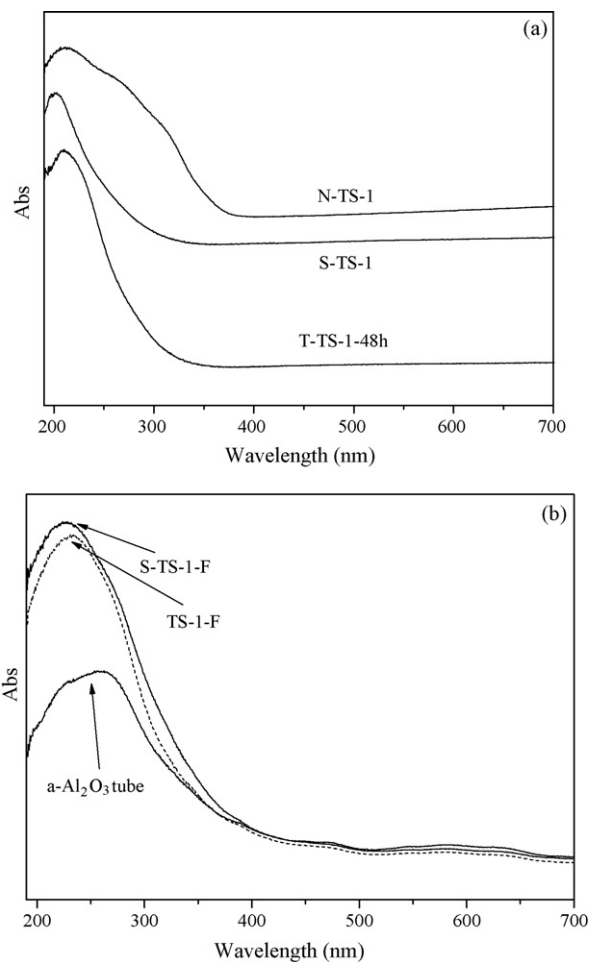


Fig. 5. UV–vis spectra of the TS-1 zeolites (a) and films (b).

completely coated with a layer of 3 μm thick Sil-1 seeds. The seed layer smooth out the uneven ceramic surface and provides nucleation sites for the zeolite crystallization. It is clear from Fig. 6c and d that a continuous layer of TS-1 zeolite film (S-TS-1-F) is formed after the hydrothermal synthesis. A 3–4 μm thick TS-1 film was uniformly grown on the Sil-1 seeded support. The difference from the synthesis of the S-TS-1 film is that the seed layer remains after synthesis and can be clearly seen from the micrograph. This is due to the fact that the synthesis solution for the films is more dilute and less alkaline than the powder synthesis solution. The zeolite crystals grew outward from the surface of the seed layer and were well intergrown forming a smooth and uniform surface. Fig. 6e and f shows that TS-1-F film grew from TS-1 seeded support appear to be identical to that S-TS-1-F except for a few larger zeolite crystals (as shown in the ellipse with broken line). Thus, it is difficult to differentiate S-TS-1-F and TS-1-F by considering only the film microstructure.

X-ray diffraction patterns of all the samples are given in Fig. 3. As in the powder samples, the film also displays the characteristic diffraction peaks belonging to TS-1 zeolite [1] except the signal is weaker considering the films were thin. Fig. 4b shows that the infrared spectra of S-TS-1-F and TS-1-F are identical with similar infrared absorption bands at 800, 1050 and 1220 cm<sup>-1</sup> similar to that of the zeolite powders (cf. Fig. 4a). There is also a weak absorption band at around 960 cm<sup>-1</sup> for both samples although the films were thin. The UV–vis spectra of the TS-1 films (cf. Fig. 5b) are also similar with both spectra exhibiting a broad band at around 220 nm belonging to Ti in zeolite framework, but the ceramic

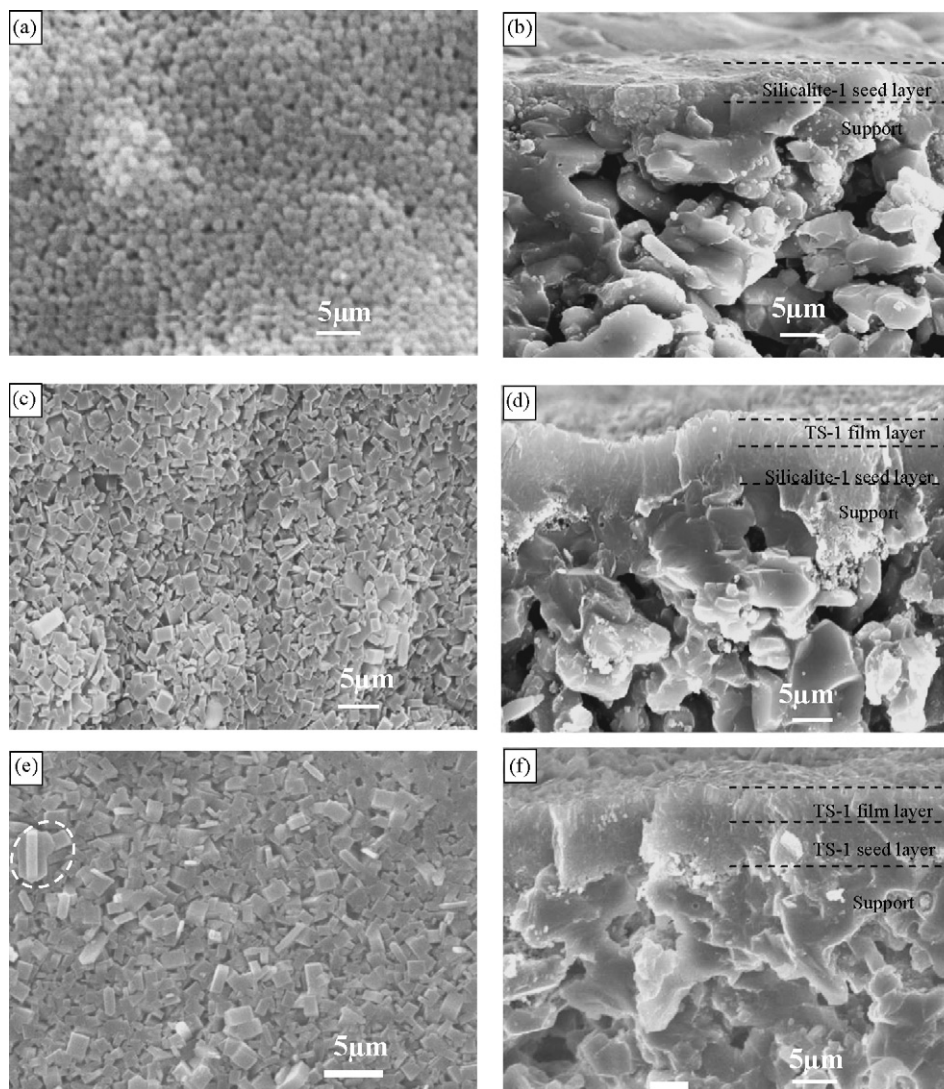


Fig. 6. SEM images of the supports seeded with Sil-1 seed (a, b); S-TS-1-F (c, d) and TS-1-F (e, f).

support also shows a similar broad band in the same region (ca. 220–270 nm). There are no obvious absorption bands in the regions around 270–280 nm and 330 nm in the films indicating that there are none or only trace amount of hexa-coordinated Ti atoms (i.e., extra-framework  $\text{TiO}_2$ ). This shows that the S-TS-1 films prepared from Sil-1 seeds is structurally and spectroscopically similar to TS-1 films prepared from TS-1 seeds.

### 3.2. Catalytic property

TS-1 zeolite catalyzes the oxidation of styrene by  $\text{H}_2\text{O}_2$  to phenylacetaldehyde (PAC) and benzaldehyde (BAL), which are both important aromatic aldehydes (AA). Table 1 summarizes the reaction performance of TS-1 zeolites and films prepared from different seeds. The conversion of styrene on the S-TS-1 zeolite prepared from Sil-1 seeds was 23% nearly twice that of N-TS-1 zeolite nucleated and crystallized from the synthesis solution. The conversion for the S-TS-1 is similar to that of the T-TS-1. The S-TS-1 is also more selective for the aromatic aldehydes, in particular for phenylacetaldehyde. Fig. 7 shows the catalytic activity over S-TS-1 powder catalyst with reaction time. The conversion of styrene and selectivity of phenylacetaldehyde on the S-TS-1 zeolites increased from 4.82% to 23% and 59.3% to 69% with increasing reaction time from 1 to 5 h, respectively. S-TS-1 and N-TS-1

are structurally and morphologically similar as indicated by the SEM and XRD data in Figs. 2 and 3. The poorer selectivity of N-TS-1 is attributed to the extra-framework Ti in this catalyst. It is well established that the extra-framework titanium species

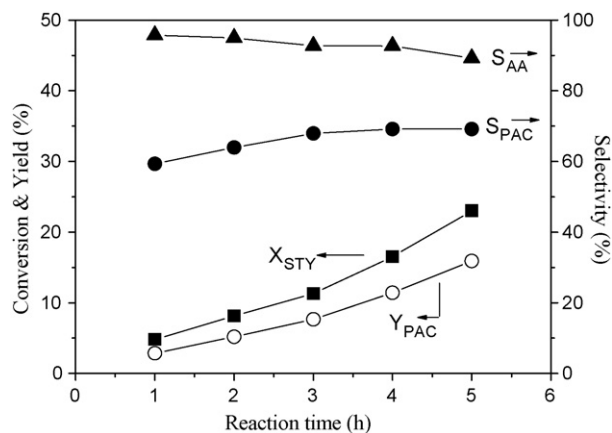


Fig. 7. The reaction results with reaction time on S-TS-1 catalyst. ■ the conversion of styrene, ▲ the selectivity of AA, ● the selectivity of PAC, ○ the yield of PAC.

**Table 1**

The catalytic properties of the TS-1 zeolites and the films.

Catalyst	Weight (g) <sup>a</sup>	Reaction time (h)	$X_{\text{STY}}$ (mol %)	Reaction rate (mmol g <sup>-1</sup> h <sup>-1</sup> )	$S_{\text{AA}}$ (mol %)	Product selectivity (mol %)		
						BAL	PAC	Others
N-TS-1	0.814	5	11.4	2.3	80	46	34	20
T-TS-1	0.814	5	24	4.8	77	3	74	23
S-TS-1	0.814	5	23	4.6	85	16	69	15
TS-1-F	0.020	1	0.27	11.1	93	40	53	7
S-TS-1-F	0.019	1	0.31	13.4	100	47	53	0

Reaction conditions: 343 K, 27.8 ml acetone, 9.415 ml styrene and 2.785 ml 30% H<sub>2</sub>O<sub>2</sub>. $X_{\text{STY}}$ : the styrene conversion calculated by Eq. (1). $S_{\text{AA}}$ : the sum of the selectivity of benzaldehyde (BAL) and phenylacetaldehyde (PAC).

N-TS-1, T-TS-1, S-TS-1: TS-1 zeolite without and with TS-1 and silicalite-1 seeds.

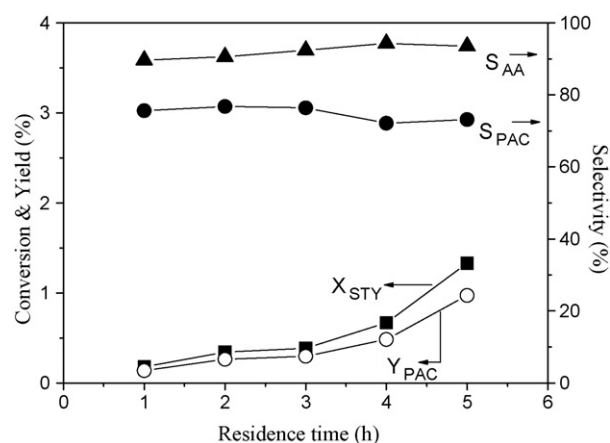
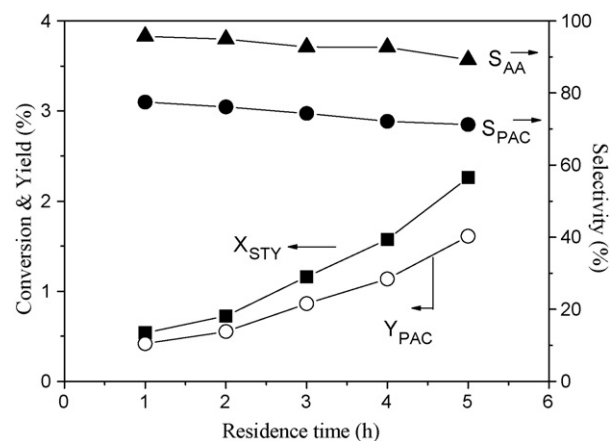
TS-1-F, S-TS-1-F: TS-1 film from TS-1 seeds and silicalite-1 seeds, respectively.

<sup>a</sup> For film catalyst loading: the weight of Sil-1 seeds was excluded, but the weight of TS-1 seeds was included in reaction measurement, as the former is inert.

decompose hydrogen peroxide [41] and catalyze carbon–carbon bond cleavage resulting in the higher benzaldehyde yield [42]. The reaction study clearly showed that TS-1 prepared from Sil-1 seeds is active for partial oxidation of styrene and has better reaction performance than TS-1 zeolites crystallized by traditional method.

Table 1 also lists the reaction over S-TS-1-F and TS-1-F films prepared from Sil-1 and TS-1 seeds, respectively. Both films are structurally and chemically identical and display similar reaction performance. The film catalysts are selective for aromatic aldehydes with slightly higher selectivity for phenylacetaldehyde than for benzaldehyde. S-TS-1-F appears to be slightly more selective than TS-1-F. The film catalysts have lower conversions compared to the powder catalysts. This is because the film catalysts weights 1/40 that of the powder catalysts used in the batch reaction. The reaction rates in term of styrene conversion indicated that the film catalysts are more reactive than the powder reactive due to lower intrinsic and external diffusion resistance.

TS-1 film catalysts of 3, 4 and 5 μm thicknesses were grown from Sil-1 seeds and used for the partial oxidation of styrene. The TS-1 films were simply grown for different lengths of time from synthesis solutions of similar composition. The amount of deposited TS-1 was weighed and the thickness was measured from the SEM cross-sections. Table 2 shows that there is weak correlation between film thickness and reaction conversion. This suggests that only the top-most layer of the film catalyst participates in the reaction due to the slow diffusion into the zeolite pores. The phenylacetaldehyde selectivity is strongly correlated to the infrared band for framework Ti–O–Si at 960 cm<sup>-1</sup>. F2 film catalyst with high  $I_{960}/I_{800}$  ratio of 2.45 has 78% selectivity for phenylacetaldehyde compared to 44% from F3 that has a low  $I_{960}/I_{800}$  of 2.25. This observation is in line with the reports by other researchers [43]. Figs. 8–10 plot the styrene partial oxidation reaction over F1, F2 and F3 film catalysts as a function of residence time, respectively. The plots were obtained from three experimental runs over the films with different thickness, respectively. The figures show a longer residence time leads to higher styrene conversion and phenylacetaldehyde yield with an overall selectivity to aromatic aldehydes better than 90%. Chen and

**Fig. 8.** The reaction results with residence time on F1 catalyst. ■ the conversion of styrene, ▲ the selectivity of AA, ● the selectivity of PAC, ○ the yield of PAC.**Fig. 9.** The reaction results with residence time on F2 catalyst. ■ the conversion of styrene, ▲ the selectivity of AA, ● the selectivity of PAC, ○ the yield of PAC.**Table 2**

Results of the oxidation of styrene over TS-1 films with different film thickness.

Catalyst	Thickness (μm)	Weight (g)	$I_{960}/I_{800}$	$X_{\text{STY}}$ (mol %)	Reaction rate (mmol g <sup>-1</sup> h <sup>-1</sup> )	Product selectivity (mol %)		
						BAL	PAC	Others
F1	3	0.019	2.33	0.31	13.4	47	53	0
F2	4	0.022	2.45	0.54	20.2	18	78	4
F3	5	0.033	2.25	0.38	9.5	45	44	11

Reaction conditions: 343 K, residence time (h)=1.

F1, F2, F3: the TS-1 films synthesized for one (S-TS-1-F), two and three times with silicalite-1 seed, respectively.

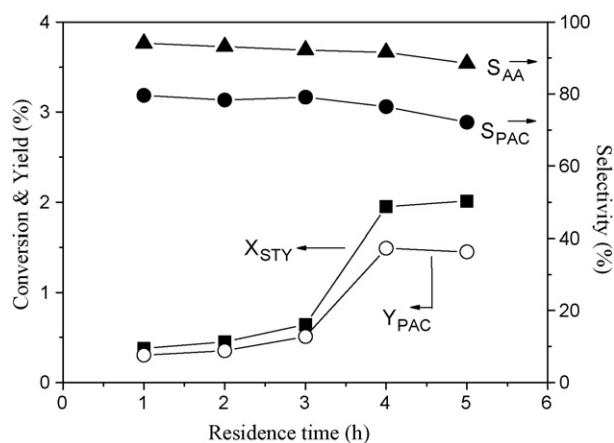


Fig. 10. The reaction results with residence time on F3 catalyst. ■ the conversion of styrene, ▲ the selectivity of AA, ● the selectivity of PAC, ○ the yield of PAC.

coworkers [44] found that polar molecules, such as the water by-product from the styrene selective oxidation reaction, react with the metal-oxygen framework of TS-1 resulting in titanium leaching and subsequent lost in selectivity and deactivation of catalyst. The reaction data in Figs. 8–10 show the film catalysts maintained a high selectivity for phenylacetaldehyde during the entire experiment.

#### 4. Conclusions

This work shows that TS-1 prepared from Sil-1 seeds are active for styrene partial oxidation reaction in spite of initial concerns that Sil-1 seeds could lead to a nonuniform or diluted catalyst. The TS-1 powder catalyst prepared from seeded synthesis is more active than the TS-1 zeolite nucleated from the synthesis solution. Seeding accelerates the crystallization of TS-1 and favors the Ti incorporation in the zeolite framework resulting in better selectivity and higher reaction conversion. TS-1 film catalysts prepared from Sil-1 and TS-1 seeds are structurally and spectroscopically identical and exhibit similar reaction performance. Only the topmost layer of the film catalyst appeared to participate in the reaction due to the slow diffusion in the zeolite pores, thus the reaction conversion is insensitive to film thickness (i.e., loading). However, phenylacetaldehyde selectivity increases with in-framework titanium content. Future work will focus on improving reaction conversion of TS-1 film catalysts without compromising selectivity. One way of obtaining higher conversion is to increase the geometric area of the catalyst by using hollow fibers and structured supports (e.g., monoliths). A microreactor will afford similar advantages, while simultaneously eliminating external mass transfer. Also depositing a rougher catalyst film with less crystal intergrowth on the microchannel is expected to allow faster diffusion.

#### Acknowledgements

The authors gratefully acknowledge the financial support from the National Natural Sciences Foundation of China (NNSF) (Grant no. 20673017) and PetroChina Innovation Fundation (Grant no. 2008D-5006-05-06).

#### References

- [1] M. Taramasso, G. Perego, B. Notari, US Patent 4,410,501 (1983).
- [2] N. Phonthammachai, M. Krissanasaeernee, E. Gulari, A.M. Jamieson, S. Wongkasemjit, Mater. Chem. Phys. 97 (2006) 458.
- [3] A.J.H.P. Van der Pol, A.J. Verduyn, J.H.C. Van Hooff, Appl. Catal. A: Gen 92 (1992) 113.
- [4] Y.S.S. Wan, J.L.H. Chau, A. Gavriilidis, K.L. Yeung, J. Catal. 223 (2004) 241.
- [5] A.J.H.P. Van der Pol, J.H.C. Van Hooff, Appl. Catal. 92 (1992) 93.
- [6] X.W. Guo, G. Li, X.F. Zhang, X.S. Wang, Stud. Surf. Sci. Catal. 112 (1997) 499.
- [7] H.H. Lu, Y.Q. Wang, React. Kinet. Catal. Lett. 89 (2006) 219.
- [8] M. Shibata, J. Gérard, Z. Gabelica, Micropor. Mater. 12 (1997) 141.
- [9] C.S. Cundy, J.O. Forrest, R.J. Plaisted, Micropor. Mesopor. Mater. 66 (2003) 143–156.
- [10] C.S. Cundy, J.O. Forrest, Micropor. Mesopor. Mater. 72 (2004) 67–80.
- [11] E.E. McLeary, J.C. Jansen, F. Kapteijn, Micropor. Mesopor. Mater. 90 (2006) 198.
- [12] R. Dittmeyer, V. Hollein, K. Daub, J. Mol. Catal. A 173 (2001) 135.
- [13] K.L. Yeung, R. Aravind, R.J.X. Zawada, J. Szeigner, G. Cao, A. Varma, Chem. Eng. Sci. 49 (1994) 4823.
- [14] V. Meille, Appl. Catal. A: Gen 315 (2006) 1.
- [15] M.A. Urbiztondo, E. Valera, T. Trifonov, R. Alcubilla, S. Irusta, M.P. Pina, A. Rodríguez, J. Santamaría, J. Catal. 250 (2007) 190.
- [16] J.L.H. Chau, Y.S.S. Wan, A. Gavriilidis, K.L. Yeung, Chem. Eng. J. 88 (2002) 187.
- [17] S.M. Lai, C.P. Ng, R. Martin-Aranda, K.L. Yeung, Micropor. Mesopor. Mater. 66 (2003) 239.
- [18] J. Coronas, J. Santamaría, Chem. Eng. Sci. 59 (2004) 4879.
- [19] X.F. Zhang, E.S.M. Lai, R. Martin-Aranda, K.L. Yeung, Appl. Catal. A: Gen. 261 (2004) 109.
- [20] X.D. Wang, B.Q. Zhang, X.F. Liu, J.Y.S. Lin, Adv. Mater. 18 (2006) 3261.
- [21] L.T.Y. Au, J.L.H. Chau, C.T. Ariso, K.L. Yeung, J. Membr. Sci. 183 (2001) 269.
- [22] Y.S.S. Wan, J.L.H. Chau, A. Gavriilidis, K.L. Yeung, Chem. Commun. (2002) 878.
- [23] X.S. Chen, P. Chen, H. Kita, Micropor. Mesopor. Mater. 115 (2008) 164.
- [24] Y.S.S. Wan, K.L. Yeung, A. Gavriilidis, Appl. Catal. A: Gen. 281 (2005) 26.
- [25] L.C. Boudreau, J.A. Kuck, M. Tsapatsis, J. Membr. Sci. 152 (1999) 41.
- [26] W.C. Wong, L.T.Y. Au, P.S. Lau, C. Tellez, K.L. Yeung, J. Membr. Sci. 193 (2001) 141.
- [27] Z. Lai, M. Tsapatsis, J.P. Nicolich, Adv. Funct. Mater. 14 (7) (2004) 716.
- [28] X.F. Zhang, H.O. Liu, A.J. Wang, J.Q. Wang, Front. Chem. Eng. China 1 (2007) 172.
- [29] L.T.Y. Au, K.L. Yeung, J. Membr. Sci. 194 (2001) 33.
- [30] E. Dincer, A. Culfaz, H. Kalipcilar, Desalination 200 (2006) 66.
- [31] X.F. Zhang, H.O. Liu, K.L. Yeung, Mater. Chem. Phys. 96 (2006) 42.
- [32] E.S.M. Lai, L.T.Y. Au, K.L. Yeung, Micropor. Mesopor. Mater. 54 (2002) 63.
- [33] G.Y. Zhang, J. Sterte, B.J. Schoeman, Chem. Mater. 9 (1997) 210–217.
- [34] L.Q. Wang, X.S. Wang, X.W. Guo, G. Li, J.H. Xiu, Chin. J. Catal. 22 (2001) 513.
- [35] M.C. Capel-Sanchez, J.M. Campos-Martin, J.L.G. Fierro, Appl. Catal. A: Gen. 246 (2003) 69.
- [36] N.G. Vayssilov, Catal. Rev. Sci. Eng. 39 (1997) 209.
- [37] M. Bandyopadhyay, A. Birkner, M.W.E. van den Berg, K.V. Klementiev, W. Schmidt, W. Grunert, H. Gies, Chem. Mater. 17 (2005) 3820.
- [38] T. Blasco, M.A. Cambor, A. Corma, J. Pérez-Pariente, J. Am. Chem. Soc. 115 (1993) 11806.
- [39] G. Li, X.W. Guo, X.S. Wang, G.Y. Li, Q. Zhao, X.H. Bao, L.W. Lin, Chin. J. Fuel Chem. Tech. 27 (1999) 565.
- [40] M. Tamura, W. Chaikittisilp, T. Yokoi, T. Okubo, Micropor. Mesopor. Mater. 112 (2008) 202.
- [41] J.Q. Zhuang, D. Ma, Z.M. Yan, X.M. Liu, X.W. Han, X.H. Bao, Y.H. Zhang, X.W. Guo, X.S. Wang, Appl. Catal. A: Gen. 258 (2004) 1.
- [42] Q.H. Yang, C. Li, S.D. Yuan, J. Li, P.L. Ying, Q. Xin, W.D. Shi, J. Catal. 183 (1999) 128.
- [43] G. Ovejero, R. van Grieken, M.A. Uguina, D.P. Serrano, J.A. Melero, J. Mater. Chem. 8 (1998) 2269.
- [44] L.Y. Chen, G.K. Chuah, S. Jaenicke, J. Mol. Catal. A 132 (1998) 281.